RSC Advances

ROYAL SOCIETY OF CHEMISTRY

www.rsc.org/advances

An efficient approach to explore the adsorption of benzene and phenol on the nanostructured catalysts: A DFT analysis

Soheila Javadian,* Fatemeh Ektefa

Correspondence to: S. Javadian; E-mail: javadian_s@modares.ac.ir, javadians@yahoo.com; Fax: +98-21-82883455

Department of Physical Chemistry, Tarbiat Modares University, P.O. Box 14115-117, Tehran, Iran

ABSTRACT

Adsorption of benzene and phenol on the 8T cluster model of ZSM-5 and Al-ZSM-5 catalysts, defined as $((H)_3SiO)_3$-Si-O-Si-$(OSi(H)_3)_3$ and $((H)_3SiO)_3$-Si-O(H)-Al-$(OSi(H)_3)_3$ structures, respectively, has been investigated comparatively using B3LYP, M06-2X, and *w*B97XD functionals employing 6-311++G** standard basis set. Geometric parameters predict one and two types of hydrogen bondings in the guest-ZSM-5 and guest-Al-ZSM-5 complexes, respectively. Variations of adsorption energy, isotropic chemical shifts, δ_{iso}, of ^{1}H, ^{17}O, ^{27}Al, and ^{29}Si atoms contributing in the hydrogen bonding as well as quadrupole coupling constant, C_Q, and asymmetry parameter, η_Q, of ^{2}H, ^{17}O, and ^{27}Al atoms have been well correlated with the strength of hydrogen bonds. Atom in Molecules (AIM) calculations showed a covalent nature for hydrogen bonds in the phenol…Al-ZSM-5 adsorption complex. Furthermore, based on AIM, NQR and NMR, the C-H…O and O-H…л hydrogen bonds have been confirmed in the benzene adsorbate zeolite, which may highlight a crucial feature of the adsorption of benzene molecule inside the pores of zeolite. The differences in the adsorption behavior between benzene and phenol on the ZSM-5 and Al-ZSM-5 are attributed to the differences in the strength of hydrogen bonding interactions. Finally, Al-ZSM-5 appears to be an efficient adsorbent for phenol and benzene.

Keywords: ZSM-5, DFT, NMR, NQR, QTAIM

INTRODUCTION

Zeolites, which are employed in a wide range of important petroleum and petrochemical processes as adsorbents and are the most important heterogeneous catalysts for separation of hydrocarbons and other processes, are crystalline, nano porous molecular sieves. They owe their extensive applicability to their unique characteristics such as tunable acidity, high surface area, uniform pore size, and good thermal/mechanical stability [1]. ZSM-5 catalysts are one of the most valuable catalysts with MFI-type topology. They are crystalline aluminosilicates with high silica to alumina ratio, based on frameworks with periodic arrangements of channels or pores, widely used in the chemical industries including petroleum refining. ZSM-5 network consists of two sets of intersecting 10-ring channel systems, running perpendicular to each other: straight circular (0.53 × 0.56 nm in diameter) and sinusoidal elliptical (0.51 × 0.55 nm in diameter) channels. Trivalent Al substitutions in the tetravalent Si framework cause the acidity of this framework structure, leading to a charge imbalance. The charge imbalance, which is compensated with a counter ion, is centered on a bridging oxygen atom located between aluminum and silicon atoms. When the counter ion is a proton, a Brönsted acid site, available for catalytic reactions is formed [2, 3].

Probing the type of interaction between guest molecule and ZSM-5 is of great importance because a lot of industrially important processes begin with the adsorption of guest molecules inside the pores of the ZSM-5. Therefore, adsorption of guest molecules, especially hydrocarbons in the ZSM-5, is widely considered experimentally and theoretically [4-10]. Similar dimensions of zeolite channels to the diameter of benzene molecule (0.58 nm) as well as the acid sites in MFI framework makes the adsorption of aromatic hydrocarbons in MFI type zeolites particularly interesting. Adsorption of aromatic hydrocarbons such as benzene and phenol is

significant. Benzene is directly oxidized to phenol using ZSM-5 type zeolite and nitrous oxide as the catalyst and oxidizing agent, respectively, as an alternative to the traditional cumene process. Good performance of [Al] MFI in selective oxidation of benzene to phenol has been reported by Hensen *et al.* [6-9, 11]. The adsorption of basic probe molecules is mostly based on the formation of hydrogen bonding between the ZSM-5 and guest molecule and formation of A…B adducts, where A and B are ZSM-5 and weak base, respectively. C-H…O and O-H…л bonds are well considered as hydrogen bonds which are associated with unconventional donor/acceptor functional group [12-14]. C-H could be a hydrogen bond donor concerning C-H…O hydrogen bonds according to Huggins's suggestion in 1936 [15]. In addition, given a potential relevance to heterogeneous catalysis, O-H…л hydrogen bond has attracted the interest of chemists. Electrons could function as hydrogen bond acceptors under some circumstances. The structural influence and functional relevance of hydrogen bonds by the application of a variety of experimental and theoretical means are still subject to hot debates among material scientists, biochemists, and others interested in fundamental structure/property issues [16]. Thus, valuable information regarding adsorption process of guest molecules can be provided by the determination of hydrogen bonds and comparison of their strength. In order to explore the electronic structure of compounds, several spectroscopic methods such as solid state nuclear magnetic resonance (NMR) and nuclear quadrupole resonance (NQR) spectroscopy have been employed. NQR spectroscopy is one of the very sensitive of these techniques to characterize the electronic environment and reveal the details of charge distribution around the nuclei with spin angular momentum of over one half ($I > 1/2$) [17-19]. Another powerful, high potential tool for the exploration of the local electronic structure of framework atoms in the solid catalysts is based on solid state NMR spectroscopy, which offers invaluable evidence about the electrostatic

interactions [20, 21]. Hydrogen bondings, at the other extreme, can be described as far as delocalization (or charge transferring) effects are concerned. These suggest a covalent nature for these interactions [22].

Despite several studies on adsorption of benzene and phenol on ZSM-5 zeolite [23-27], few detailed computational works have considered the type of interaction between benzene and phenol with ZSM-5 host lattice through NMR, NQR, and AIM analysis. Our understanding of adsorption process of aromatic hydrocarbons may be facilitated by the investigation of interactions and comparison of strength of these complexes. Importantly, we are interested in the explanation of the nature and consequences of hydrogen bonds. The type of interactions and relationship between alternation of spectroscopic parameters and strength of hydrogen bondings are revealed by quantum chemical calculations. We have systematically implemented a quantum mechanical investigation of charge distribution on the benzene and phenol adsorbate complex on the solid acids of different strengths including ZSM-5 and Al-ZSM-5 zeolites by the application of NMR and NQR parameters as well as Natural Bond Orbital (NBO) and quantum theory of atoms in molecules (QTAIM) analysis to reach this purpose. Combination of nuclear magnetic resonance (NMR) and nuclear quadrupole resonance (NQR) techniques thus presents a powerful tool for the investigation of the type of interactions in the adsorption complexes and successful interpretation of the observed results. NBO and QTAIM analyses finally complete the structural analysis.

COMPUTATIONAL PROCEDURE

Zeolite cluster models

The cluster models are presumed based on the crystallographic coordinates of ZSM-5 zeolites reported by van Koningsveld *et al.* [28]. It is compulsory to model unit cell of ZSM-5

zeolite with 288 atoms (96 silicon and 192 oxygen atoms) to obtain reliable results. Modeling of a large unit cell of ZSM-5 zeolite is, nevertheless, computationally expensive. Thus, a fragment of appropriate size from the zeolite framework must be chosen. Clusters containing eight tetrahedral centers are reliable models compared to experimental results, as indicated by previous works [29-31]. This fragment of zeolite framework includes the intersection of the straight and sinusoidal channels which is accessible to the interaction between bridging hydroxyl group and guest molecules as a catalytic active site. Therefore, in the present study, the clusters containing eight tetrahedral centers (8T), defined as $((H)_3SiO)_3$-Si-O-Si-$(OSi(H)_3)_3$ and $((H)_3SiO)_3$-Si-O(H)-Al-$(OSi(H)_3)_3$ structures, in which one of the Si sites had been substituted by an Al atom in the latter, were chosen. In order to obtain a neutral cluster, the boundary Si atoms were saturated with hydrogen atoms. Cluster models are referred to as 8T-ZSM-5 and 8T-Al-ZSM-5, respectively, from here on for the sake of brevity.

Theoretical background and methods of analysis

GAMESS program package has been used to carry out all quantum mechanical calculations in this work [32]. B3LYP, M06-2X, and *w*B97XD functionals in conjugation with 6-311++G** basis set that contains polarization and diffuse functions on all atoms has been applied to perform geometry optimization of benzene and phenol adsorbate complexes. B3LYP has been selected as a conventional functional has been widely used in literature. Additionally, M06 and *w*B97XD have been used as specifically parameterized functionals for systems having dominant weak dispersive interactions in order to improve the description of noncovalent and π-stacking interactions. Specially, M06-2X has been employed to explore the zeolite-catalyzed reactions [33-36]. Coordinates of all atoms in the cluster, excluding boundary Si and H atoms, kept fixed in their crystallographic positions, were allowed to relax throughout the geometry

optimization procedure. The optimized cluster models have been subjected to chemical shielding (CS) and electric field gradient (EFG) tensors at the as well as NBO and QTAIM analyses.

A traceless, second-rank tensor, whose principal components are defined as $|q_{zz}| \geq |q_{yy}| \geq |q_{xx}|$, can be used to describe the EFG. Two other experimentally measurable NQR parameters include the nuclear quadrupole coupling constant, C_Q, and its associated asymmetry parameter, η_Q. The amount of interaction energy between the electric quadrupole moment, eQ, of the nucleus and the EFG at the quadrupole nucleus site due to the anisotropic charge distribution in the system can be shown by C_Q. This gives information regarding electron distribution in the molecule and is defined as [17, 37]:

$$C_Q(\text{MHz}) = e^2Qq_{zz}/h \quad (1)$$

where e is the electron charge and h is the Planck constant. The standard values of Q were employed as Q(^{2}H) = 2.86 mb, Q(^{17}O) = 25.58, and Q(^{27}Al)=146.6 mb, as reported by Pyykkö [38]. The deviation of EFG tensors from cylindrical symmetry at the site of quadrupolar nucleus is measured by asymmetry parameter, η_Q, using equation (2):

$$\eta_Q = |q_{yy}-q_{xx}|/ |q_{zz}|, \ 0 \leq \eta_Q \leq 1 \quad (2)$$

To carry out chemical shielding calculations, the gauge independent atomic orbital (GIAO) [39] method was employed. The chemical shielding tensor is one of the important NMR parameters, which shows the magnetic shielding effect of electrons, especially valence electrons around atomic nucleus. $\sigma_{33} > \sigma_{22} > \sigma_{11}$ are defined as the three principal components of the corresponding CS tensor. The chemical shielding isotropy, σ_{iso}, is used in addition to the three principal components, $\sigma_{iso}= (\sigma_{33} + \sigma_{22} + \sigma_{11})/3$ to describe a CS tensor. The predicted ^{1}H and ^{29}Si, ^{17}O, and ^{27}Al chemical shifts (in ppm) are derived from equation $\delta_{iso}= \sigma_{iso,ref} - \sigma_{iso,cal}$, in which $\sigma_{iso,cal}$ is the absolute shielding and $\sigma_{iso,ref}$ refers to the absolute chemical shielding of

tetramethylsilane (TMS), liquid water and chabasite, respectively [20, 40-42]. Natural Bond Orbital (NBO) analysis [43] used to calculate natural charges for cluster models were performed on wave functions calculated at the M06-2X/6-311++G** level. AIM2000 package was used to implement the AIM analysis for cluster models considered at the M06-2X/6-311++G** computational level [44].

Finally, for each cluster, the adsorption energy ΔE_{ads} of benzene and phenol on the zeolites has been calculated which is defined as the energy difference between the complex system and the sum of the separated fragments.

RESULTS AND DISCUSSION

For the purpose of clarity, this part of the work is divided into three different subdivisions including geometry, NMR and NQR, NBO and AIM parameters.

Geometrical aspects of adsorption

The geometries and hydrogen bonds of the optimized adsorption complexes at M06-2X/6-311++G** are depicted in Fig. 1. The calculated bond lengths and angles between the most important atoms of these cluster models, as well as full details of geometrical parameters of hydrogen bonds are summarized in Table 1. Throughout this work, Z, P and B subscripts denote zeolite, phenol and benzene, respectively.

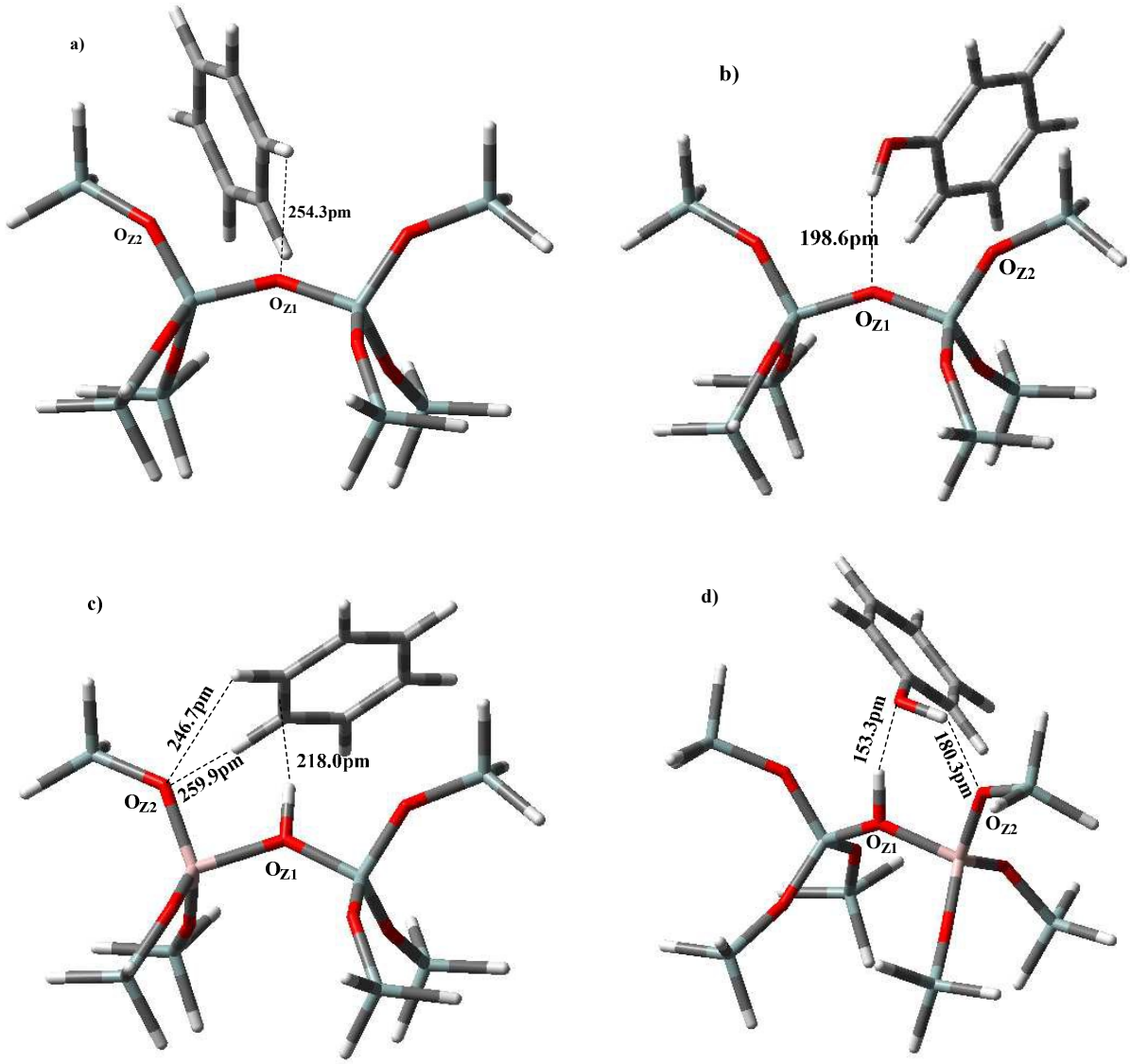

Fig. 1. Representation of hydrogen bonding interactions in: a)8T-ZSM-5…Benzene, b)8T-ZSM-5…Phenol, c)8T-Al-ZSM-5…Benzene, and d)8T-Al-ZSM-5…Phenol cluster models at M06-2X/6-311++G** level.

Table 1

Selected optimized geometrical parameters (bond lengths in pm and angles in degrees) of the cluster models before and after adsorption calculated at the M06-2X/6–311++G**level of theory. The values in parentheses represent the data before adsorption.

Cluster models							
8T-ZSM-5 …Benzene		8T-ZSM-5 …Phenol		8T-Al-ZSM-5 …Benzene		8T-Al-ZSM-5 …Phenol	
$d(C_B\text{-}H_B)$	108.4 (108.4)	$d(C_P\text{-}O_P)$	135.3 (136.3)	$d(C_B\text{-}H_B)$	108.5 (108.4)	$d(C_P\text{-}O_P)$	139.0 (136.3)
$d(Si\text{-}O_{Z1})$	160.2 (159.7)	$d(O_P\text{-}H_P)$	96.7 (96.1)	$d(Al\text{-}O_{Z1})$	181.2 (182.4)	$d(O_P\text{-}H_P)$	98.1 (96.1)
$d(Si\text{-}O_{Z2})$	159.5 (159.9)	$d(Si\text{-}O_{Z1})$	161.5 (159.7)	$d(Al\text{-}O_{Z2})$	169.0 (168.9)	$d(Al\text{-}O_{Z1})$	180.2 (182.4)
$\angle(O_{Z1}\text{-}M\text{-}O_{Z2})$	104.1 (104.9)	$d(Si\text{-}O_{Z2})$	159.2 (159.9)	$d(O_{Z1}\text{-}H_Z)$	97.7 (96.9)	$d(Al\text{-}O_{Z2})$	170.9 (168.9)
$d(C_B\text{-}H_B\ldots O_{Z1})$	254.3	$\angle(O_{Z1}\text{-}M\text{-}O_{Z2})$	103.8 (104.9)	$\angle(O_{Z1}\text{-}M\text{-}O_{Z2})$	91.7 (90.5)	$d(O_{Z1}\text{-}H_Z)$	102.5 (96.9)
$\angle(C_B\text{-}H_B\ldots O_{Z1})$	117.5	$d(O_P\text{-}H_P\ldots O_{Z1})$	198.6	$d(C_B\text{-}H_B\ldots O_{Z2})$	246.7	$\angle(O_{Z1}\text{-}M\text{-}O_{Z2})$	92.8 (90.5)
		$\angle(O_P\text{-}H_P\ldots O_{Z1})$	161.0	$\angle(C_B\text{-}H_B\ldots O_{Z2})$	116.5	$d(O_{Z1}\text{-}H_Z\ldots O)$	153.3
				$d(C_B\text{-}H_B\ldots O_{Z2})$	259.9	$\angle(O_{Z1}\text{-}H_Z\ldots O)$	161.8
				$\angle(C_B\text{-}H_B\ldots O_{Z2})$	111.8	$d(O_P\text{-}H_P\ldots O_{Z2})$	180.3
				$d(O_{Z1}\text{-}H_Z\ldots л)$	218.0	$\angle(O_P\text{-}H_P\ldots O_{Z2})$	140.9
				$\angle(O_{Z1}\text{-}H_Z\ldots л)$	155.8		

It can be concluded that bond distances such as benzene C–H and that of the acidic hydroxyl group of the isolated Al-ZSM-5 cluster model are in excellent agreement with the experimental observation of 108.4 and 97.5 pm, respectively [45, 46].

It should be pointed out that for the analysis of the interaction of benzene and phenol with the zeolite, initial geometry was started where benzene and phenol were assumed at the center, with benzene ring oriented approximately perpendicular to the plane of the zeolite. These orientations are approximately preserved for 8T-ZSM-5 adsorption complex after optimization whereas for 8T-Al-ZSM-5 adsorption complex, the aromatic ring of benzene and phenol were moved approximately parallel to the plane of the zeolite. It's noteworthy that optimizations of different initial orientations of complexes resulted in conformations as reported. These conformations correspond to the best orientation, based on creating most interactions resulting in most stable configuration, and are in good agreement with similar previous studies [29, 31].

Fig. 1 and the results of Table 1 show a single molecule of phenol interacts with the site of 8T-ZSM-5 and 8T-Al-ZSM-5 zeolite frameworks via one and two type of hydrogen bonds, respectively. In the latter, the oxygen atom of phenol (O_P) interacts with the hydrogen of Brönsted acid (H_Z) with an $O_P…H_Z$ bond length of 153.3 pm, and another hydrogen bond is formed between the hydrogen atom of phenol (H_P) and the oxygen atom of 8T-Al-ZSM-5 framework (O_{Z2}) with an $O_Z…H_P$ bond length of 180.3 pm. Consequently, a six membered ring is formed (see Fig. 1). Based on Jeffrey's classification [47], hydrogen bonds are classified into strong, moderate and weak types, with bond lengths 120–150, 150–220 and 220–320 pm, respectively. Consequently, based on the results presented in Tables 1, $O_P…H_Z$ and $O_Z…H_P$ hydrogens are classified as moderate types. Furthermore, based on the results of Table 1 the hydrogen bond formed in the phenol…ZSM-5 adsorption complex is moderate, too. It is worth

mentioning that benzene molecule interacts with the zeolite framework via one and three hydrogen bonds in the benzene…ZSM-5 and benzene…Al-ZSM-5, respectively (see Fig. 1). In the benzene…ZSM-5 adsorption complex, hydrogen atom of benzene interacts with oxygen atom of ZSM-5 with a $H_B…O_Z$ bond length of 254.3 pm. In the latter, the hydrogen of Brönsted acid (H_Z) interacts with the л electrons of benzene with a л…H_Z-O_Z bond length of 218.0 pm and the other hydrogen bond is formed between two hydrogen atoms of benzene (H_B) and the oxygen atom of 8T-Al-ZSM-5 framework (O_{Z2}) with an $O_Z…H_B$ bond length of 253.3 pm, on average, resulting in a five membered ring. From the geometrical results, it is concluded that all the hydrogen bonds, excluding л…H_Z-O_Z, in the benzene adsorption complex are categorized as classified weak and complex formation takes place, associated with weak hydrogen bonds. These results are in good agreement with the study of Koch and Popelier, and Panigrahi *et al.* [48, 49] on the basis of weak hydrogen bonds.

Generally, Table 1 shows that geometry parameters including bonds and angles of hydrogen bonds of phenol…ZSM-5 and phenol…Al-ZSM-5 adsorption complexes are more proper than those of benzene…ZSM-5 and benzene…Al-ZSM-5 adsorption complexes. Comparison of the calculated bond lengths in Table 1 shows that the O_{Z1}–H_Z distance of the 8T-Al-ZSM-5 is elongated upon complexation. Increasing of O_{Z1}–H_Z bond length becomes higher when the guest molecule is changed from benzene to phenol (97.7 and 102.5 vs. 96.9 pm due to formation of hydrogen bonding with the benzene and phenol, respectively) confirming stronger hydrogen bonds in the phenol adsorption complex compared to benzene. It is worth mentioning that this case is well correlated with the long-range interactions. In addition the Al–O_{Z1} bond lengths decrease upon complexation with benzene and phenol by about 1.2 and 2.2 pm, respectively, whereas Si–O_{Z1} bond lengths increase. Variation of Si–O_{Z1} and Al–O_{Z1} bond

lengths becomes greater in going from benzene…zeolite to phenol…zeolite. Table 1 shows that the complexation can also affect O_{Z1}–M–O_{Z2} bond angles. O_{Z1}–Al–O_{Z2} bond angles increase whereas O_{Z1}–Si–O_{Z2} bond angles decrease. O_{Z1}–Al–O_{Z2} bond angle, acting as adsorption sites in the 8T-Al-ZSM-5 adsorption complexes, is observed to open up due to benzene and phenol adsorption. O_P–H_P bond length increase upon complex formation. In addition, benzene adsorption causes a slight elongation of C_B–H_B bond compared to the isolated molecule.

Also, B3LYP and *w*B97XD functionals in combination with 6-311++G** basis sets were used to optimize adsorption complexes. The geometrical parameters of hydrogen bonds of the optimized adsorption complexes at B3LYP/6-311++G** and *w*B97XD/6-311++G** are listed in Table S1 of Supporting Information. As seen from Table S1, the hydrogen bond lengths of adsorption complexes, especially the O_{Z1}-H_Z…л bond distance, are sensitive to the level of theory used. This indicates that dispersion may play an important role in host/guest interactions.

In the next sections, the importance of dispersive functionals has been evaluated while only the M06-2X has been selected to study the adsorption complexes as the most reliable functional to explain the host/guest interactions.

The predicted hydrogen bonds can be well elucidated with NMR, NQR, NBO and AIM parameters, which are better criteria for investigation of hydrogen bonding than the geometrical parameters. Significantly, the changes of geometrical parameters upon the adsorption of benzene, including a lengthening of the O_{Z1}–H_Z, O_P–H_P and C_B-H_B, inspired us to confirm this lengthening with the parameters mentioned. The following sections support these findings.

NMR and NQR analysis

Gauge Independent Atomic Orbital (GIAO) method employing DZVP2 basis set was implemented to confirm the predicted hydrogen bonding interactions based on NMR and NQR

parameters of absorption complexes. We examined the ability of three density functionals including B3LYP, M06-2X, and *w*P97XD to evaluate the NMR parameters. Previous studies have demonstrated that DZVP2 basis set successfully predicts the spectroscopic parameters of probe molecules adsorbed on zeolites [29, 50, 51]. We are going to mainly discuss the NMR and NQR parameters of the oxygen and hydrogen atoms of adsorption complex, which contribute to the hydrogen bonding interactions as well as Al and Si atoms at the neighboring Brönsted acid site. The calculated ^{17}O, ^{1}H, ^{27}Al and ^{29}Si chemical shielding tensors and isotropic chemical shift as well as the EFG principal components and the corresponding parameters of ^{17}O, ^{2}H, and ^{27}Al for bare and adsorption cluster models are summarized in Table 2 , respectively. Also, Tables S2-S3, in the supporting information, present the NMR and NQR parameters of mentioned atoms at the B3LYP/DZVP2 and *w*B97XD/DZVP2 levels, respectively.

Table 2

Selected calculated ^{17}O, ^{1}H, and ^{27}Al NMR chemical shifts (in ppm), quadrupole coupling constant (in MHz for ^{17}O and ^{27}Al nuclei, and KHz for ^{2}H nuclei), and asymmetry parameter for ^{17}O, ^{2}H, and ^{27}Al nuclei before and after adsorption in the cluster models at the M06-2X/DZVP2 level of theory. The values in parentheses represent the calculated data before the adsorption.

cluster models	nucleus	δ_{iso}	C_Q	η_Q
8T-ZSM-5…Benzene	H_B	8.77(8.05)	215.82(220.17)	0.06(0.06)
	O_{Z1}	68.34(56.21)	6.36(6.59)	0.25(0.21)
	O_{Z2}	5.19(1.23)	6.57(6.68)	0.29(0.24)
	Si	-80.67(-81.98)		
8T-Al-ZSM-5…Benzene	H_B	8.72(8.05)	212.86(220.17)	0.05(0.06)
	O_{Z1}	66.09(52.05)	8.34(8.89)	0.88(0.80)
	H_Z	4.31(3.96)	290.46(317.15)	0.11(0.09)
	O_{Z2}	-1.17(-10.03)	4.05(4.10)	0.75(0.74)
	Al	72.43(73.48)	19.39(21.19)	0.25(0.21)
	Si	-80.47(-80.68)		
8T-ZSM-5…Phenol	O_P	102.55(92.31)	11.01(11.43)	0.86(0.91)
	H_P	6.42(3.74)	312.13(341.92)	0.13(0.13)
	O_{Z1}	76.04(56.21)	5.92(6.59)	0.43(0.21)
	O_{Z2}	9.69(1.23)	6.48(6.68)	0.25(0.24)
	Si	-80.06(-81.98)		
8T-Al-ZSM-5…Phenol	O_P	92.60(92.31)	10.11(11.43)	0.92(0.91)
	H_P	8.29(3.74)	266.60(341.92)	0.10(0.12)
	O_{Z1}	55.32(52.05)	6.34(8.89)	0.93(0.80)
	H_Z	12.52(3.96)	168.36(317.15)	0.18(0.09)
	O_{Z2}	10.99(-10.03)	4.03(4.10)	0.76(0.74)
	Al	73.11(73.48)	15.82(21.19)	1.00(0.21)
	Si	-80.52(-80.68)		

Fig. 1 shows that there are two distinct oxygen sites in the ZSM-5, and two distinct oxygen sites and one hydrogen site in the Al-ZSM-5. Based on the calculated results, ^{17}O, ^{1}H, ^{27}Al and ^{29}Si chemical shift isotropy, δ_{iso}, are observed to change from bare to the one in the adsorption cluster models due to the participation in the intermolecular hydrogen bonding interactions. Alteration in charge density around a particular nucleus could be manifested in its NMR chemical shift. The magnitude of these variations depends on its contribution to the interactions. The ^{17}O chemical shift value of 8T-ZSM-5 (O_{Z1}) of bare cluster model is 56.21 ppm, increasing with a $\Delta\delta_{iso}$ of 12.13 and 19.83 ppm in the benzene…ZSM-5 and phenol…ZSM-5 cluster models, respectively. The ^{17}O chemical shift value of 8T-Al-ZSM-5 (O_{Z1}) of bare cluster model is 52.05 ppm and it increases about 14.04 and 3.27 ppm in the benzene…Al-ZSM-5 and phenol…Al-ZSM-5 cluster models, respectively. In spite of the stronger hydrogen bonding of phenol…Al-ZSM-5, its δ_{iso} ($^{17}O_{Z1}$) alternation is smaller than

benzene…Al-ZSM-5 as predicted through the geometry parameters. Thus, what is the origin of the observed violation in the trend of the δ_{iso} ($^{17}O_{Z1}$) of phenol…Al-ZSM-5? It seems that hydroxyl group of phenol in the phenol…Al-ZSM-5 contributes in two hydrogen bondings through O_P and H_P (Fig. 1) resulting in formation of a six membered ring. Since the phenol molecule is a stronger base probe compared to benzene, its adsorption on the Brønsted acid site will result in a much stronger proton transfer from zeolite to phenol. In fact, one could conclude that O_{Z1} acts like O_{z2} and vice versa. Formation of six membered ring has been confirmed by AIM analysis in the next section which is in good agreement with similar previous theoretical works [36, 52, 53].

Similarity, $^{17}O_{Z2}$ chemical shift values increase in the benzene…ZSM-5, phenol…ZSM-5, benzene…Al-ZSM-5, and phenol…Al-ZSm-5 adsorption complexes compared to bare cluster model confirming the contribution of ^{17}O in the hydrogen bonding in four adsorption complexes (Table 1). More alternation of chemical shift value in the phenol adsorption complexes compared to benzene adsorption complexes is attributed to the stronger interaction in the phenol adsorption complexes.

Chemical shift values are in excellent agreement with the experimental observations which are 3.6-4.3, 6-8.5, and 4 ppm for ^2H_Z, ^2H_B, and ^2H_P, respectively [54-56]. ^2H_Z chemical shift value of 8T-Al-ZSM-5 is 3.96 ppm increasing about 0.35 and a remarkable $\Delta\delta_{iso}$ 8.56 ppm relative to the one in the benzene and phenol adsorption complex, respectively. Chemical shift is further alternated due to the stronger contribution of H_z in the hydrogen bonds in the phenol adsorption complex compared with benzene adsorption complex. These results confirm high sensitivity of chemical shielding tensors to local bonding environments.

^{29}Si and ^{27}Al chemical shift values are in good agreement with the experimental results and previous studies; -112.8 and 60 ppm, respectively [42, 57, 58]. It is noteworthy that alternations of ^{29}Si and ^{27}Al chemical shift values are insignificant because of indirect contributing in hydrogen bondings.

The influence of the hydrogen bonding interactions on the ^{2}H, ^{17}O, and ^{27}Al C_Q and η_Q for the bare and adsorption cluster models is now focused on. NQR parameters of these atoms are also changed due to hydrogen bonding interactions. According to Table 2, the C_Q ($^{2}H_Z$) value decreases from 317.15 KHz for Al-ZSM-5 to 290.46 and 168.360 KHz in benzene…Al-ZSM-5 and phenol…Al-ZSM-5, respectively, whereas the corresponding values of η_Q increase. Similar to H_z, the C_Q (O_{Z1}) and C_Q (O_{Z2}) values decrease in benzene…Al-ZSM-5 and phenol…Al-ZSM-5 complexes whereas the corresponding values of η_Q increase.

Two factors control the value of q_{zz} for a quadrupolar nucleus: the charge density at the nucleus and the symmetry of EFG around the nucleus. The hydrogen bonding interactions increase the charge density at acceptor atoms. In addition, EFG is more asymmetric in atoms due to hydrogen bonding. On the other hand, if the asymmetry of EFG increases, then q_{zz} would consequently decrease. As a result, the competing effects of charge density and EFG asymmetry on C_Q offset each other, leading to only a small decrease in the C_Q values of these compounds.

It should be pointed out that Al atom do not directly contribute to the hydrogen bonding, but alternation of C_Q parameter is considerable. It can be concluded ^{27}Al NQR parameters are in good agreement with the experimental observation of C_Q=16 MHz and η_Q=0.1[58]. According to Table 2, the C_Q (^{27}Al) value decreases about 1.80 MHz and remarkable ΔC_Q = 4.63 MHz in the benzene…Al-ZSM-5 and phenol…Al-ZSM-5, respectively. All the results are in good agreement

with geometry and NMR parameters discussed in the previous sections. In the next section, we intend to confirm our results with NBO and AIM calculations.

QTAIM and NBO analysis

To gain insight into the nature of interaction between benzene and zeolite as well as phenol and zeolite, the Bader's quantum theory [59] of atoms in molecules (QTAIM) has been applied at M06-2X/6-311++G** level. The total electronic density, $\rho(r_c)$, the Laplacian of electron density, $\nabla^2\rho(r_c)$, and total energy density (H) at the Bond Critical Points (BCPs) and Ring Critical Point (RCP), are summarized in Table 3. The hydrogen bond energies are listed in Table 4.

A shared interaction such as lone pairs and covalent bonds is shown by a negative Laplacian whereas positive Laplacian indicates where the electron density is declining as in ionic, hydrogen bonds, and van der Waals interactions.

For equilibrium molecular geometry, the molecular graphs (including the critical points and bond paths of interacting atoms) for the adsorbate complexes are presented in Fig. 2. Inspection of molecular graphs indicates that for $O_{Z1}\ldots H_B$, $O_{Z2}\ldots H_B$, $H_Z\ldots$л, $O_{Z1}\ldots H_P$, $O_{Z2}\ldots H_P$ and $H_Z\ldots O_P$, there are corresponding bond paths and critical points (CPs) within the equilibrium structures, confirming the interaction between benzene, phenol and zeolite. Another useful characterization of hydrogen bonding is the Ring Critical Point (RCP) in the resonance assisted hydrogen bonds as an important criterion to describe the hydrogen bonding. Molecular graphs of phenol…Al-ZSM-5 indicate the existence of RCP assisted $O_{Z2}\ldots H_P$ and $H_Z\ldots O_P$ hydrogen bonds which confirms the formation of six membered ring. According to the third column in Table 3, for all adsorption complexes, Laplacian of total electronic densities at BCPs of $O_{Z1}\ldots H_B$, $O_{Z2}\ldots H_B$, $H_Z\ldots$л, $O_{Z1}\ldots H_P$, $O_{Z2}\ldots H_P$ and $H_Z\ldots O_P$, are positive at the critical points,

confirming predicted hydrogen bonds. The greater $\rho_{A\cdots B}$ values correspond to stronger hydrogen bond. Thus, phenol…Al-ZSM-5 forms the strongest interaction among adsorption complexes. Weak hydrogen bonds ($E_{HB} < 50$ kJ/mol) show both $\nabla^2\rho(r_c)$ and $H_{BCP} > 0$, and medium hydrogen bonds ($50 < E_{HB} < 100$ kJ/mol) show $\nabla^2\rho(r_c) > 0$ and $H_{BCP} < 0$, as reported by Rozas *et al.*[60], whereas strong hydrogen bonds ($E_{HB} > 100$ kJ/mol) show both $\nabla^2\rho(r_c)$ and $H_{BCP} < 0$. Espinosa-Molins- Lecomte [61] formula was applied to evaluate hydrogen bond energies for all of the adsorption complexes being investigated based on the electron density distribution at the BCPs: $E_{HB} = 0.5$ V(r). The energy of $O_{Z2}\cdots H_P$ and $H_Z\cdots O_P$ hydrogen bonding interactions are 40.10 and 87.90 kJ/mol, respectively, and are classified as nearly medium and medium hydrogen bonds of partially covalent nature. The energy of C–H ⋯O and C-H…л hydrogen bonds are less than 50 kJ/mol (8.72 and 11.00 kJ/mol for C–H ⋯O and 11.70 kJ/mol for O-H…л in the 8T-Al-ZSM-5…Benzene and 8.64 kJ/mol for C–H ⋯O in the 8T-ZSM-5…Benzene) and are categorized as electrostatic weak hydrogen bonds. The energy of $H_Z\cdots O_P$ is 24.7 kJ/mol, which may be treated as weak hydrogen bonding.

It was reported that bonds with positive value of ρ(r) and small negative value of H(r) at BCP are termed as partially covalent in nature. For O_z-H_Z, O_P-H_P and C_B-H_B BCP, ρ(r) and H(r) are negative, indicating a covalent character. The results in Table 3 show that the electron density and its Laplacian at O_{Z1}–H_Z BCP of Al-ZSM-5 decrease upon complexation with benzene and phenol. In addition, the values of ρ(r) and $\nabla^2\rho(r)$ at O_P–H_P BCP of phenol and C_B-H_B BCP of benzene decrease upon complexation. Therefore, complexation causes a decrease in the covalent nature in all complexes. This decrease is greater in 8T-Al-ZSM-5 adsoption complex than in 8T-ZSM-5 adsoption complexes. The decrease of BCP data for phenol adsorbate complex is greater than that of benzene adsorbate complex due to stronger hydrogen bondings. According to these

results, it can be concluded that the interaction between phenol and zeolite in both model complexes is stronger than that between benzene and zeolite. In addition, the decrease in BCP data for O_{Z1}–H_Z bond is greater than that in O_P–H_P. Based on these results, it can be concluded that the interaction between oxygen of phenol and hydrogen of zeolite is stronger than that between hydrogen of phenol and zeolite oxygen. This result well correlate with hydrogen bonding length reported in Table 1. All the results are in agreement with NMR, NQR and NBO, reported in the previous sections.

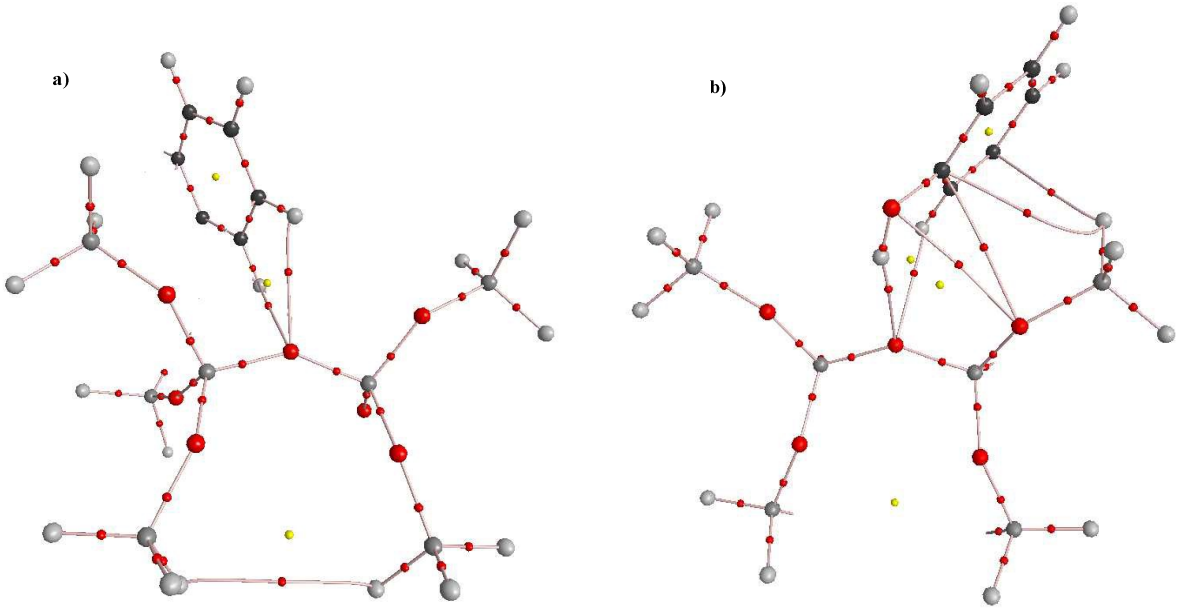

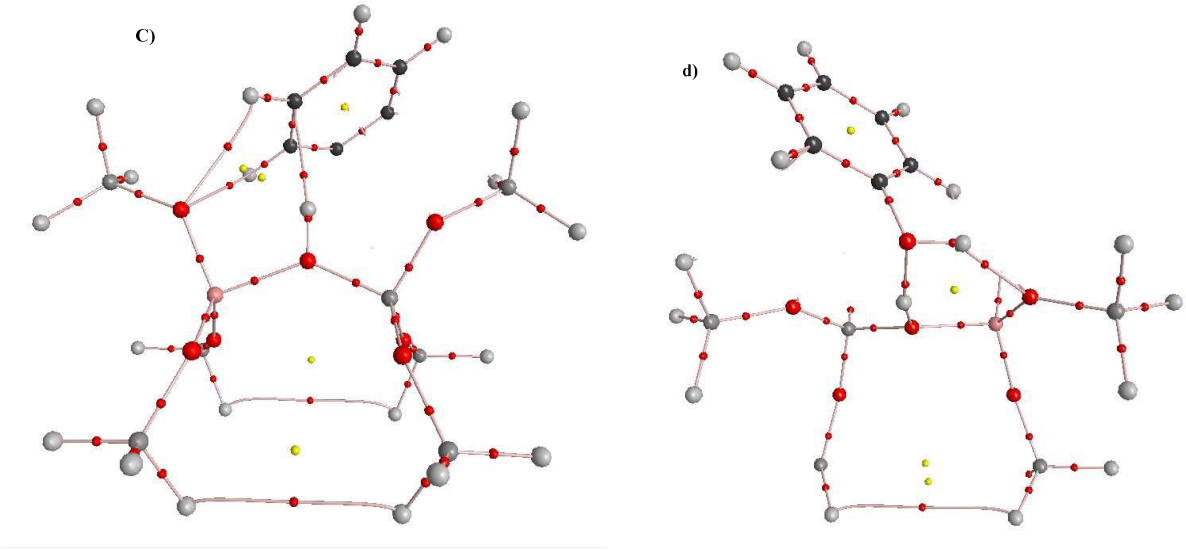

Fig. 2. Molecular graph of adsorption complexes: a)8T-ZSM-5…Benzene, b)8T-ZSM-5…Phenol, c)8T-Al-ZSM-5…Benzene and d)8T-Al-ZSM-5…Phenol. Nuclei and bond critical points are represented by big and small spheres, respectively.

Table 3

Selected calculated BCP and RCP data (au) before and after adsorption in the cluster models at the M06-2X/6-311++G** level of theory. The values in parentheses represent the data before adsorption.

Bond	ρ(r)	$\nabla^2\rho(r)$	H(r)
	8T-ZSM-5…Benzene		
C_B-H_B	0.2851(0.2838)	-1.0486(-1.0175)	-0.3009(-0.2961)
Si-O_{Z1}	0.1407(0.1422)	1.1604(1.1848)	-0.0269(-0.0273)
Si-O_{Z2}	0.1436(0.1418)	1.2000(1.1800)	-0.0285(-0.0275)
O_{Z1}…H_B	0.0093	0.0345	0.0010
	8T-Al-ZSM-5…Benzene		
C_B-H_B	0.2859(0.2838)	-1.0443(-1.0175)	-0.2998 (-0.2961)
	0.2859(0.2838)	-1.0416(-1.0175)	-0.2996(-0.2961)
O_{Z1}-H_Z	0.3304(0.3425)	-2.0714(-2.1590)	-0.5801(-0.6025)
Al-O_{Z1}	0.0709(0.0684)	0.5850(0.5598)	0.0123(0.0121)
Al-O_{Z2}	0.1019(0.1027)	0.9420(0.9494)	0.0108(0.0104)
H_Z…л	0.0155	0.0428	0.0009
O_{Z2}…H_B	0.0116	0.0409	0.0009
	0.0098	0.0352	0.0011
	8T-ZSM-5…Phenol		
O_P-H_P	0.3552 (0.3675)	-2.1600(-2.150)	-0.6094 (-0.6132)
Si-O_{Z1}	0.1366(0.1422)	1.1031(1.1848)	-0.0257(-0.0273)
Si-O_{Z2}	0.1448(0.1418)	1.2120(1.1800)	-0.0291(-0.0275)
O_{Z1}…H_P	0.0223	0.0697	-0.0007

	8T-Al-ZSM-5…Phenol		
O_P-H_P	0.3370(0.3675)	-2.0700 (-2.150)	0.5832 (-0.6132)
O_{Z1}-H_Z	0.2797(0.3425)	-1.4844(-2.1590)	0.4443(-0.6025)
Al-O_{Z1}	0.074(0.0684)	0.6084(0.5598)	0.0116(0.0121)
Al-O_{Z2}	0.0971(0.1027)	0.8776(0.9494)	0.0111(0.0104)
H_Z…O_P	0.0700	0.1419	-0.0157
O_{Z2}…H_P	0.0357	0.1156	-0.0008
RCP	0.0147	0.0758	0.0021

Other method for prediction of hydrogen bonding is charge analysis based on Weinhold's NBO calculation [43]. The deviation of the molecule from the Lewis structure is caused by delocalization of electron density from filled (bonding or lone pair) Lewis type NBOs to other neighboring electron deficient orbitals (non-Lewis type NBOs, such as anti-bonding or Rydberg) properly oriented in a NBO representation. This can be applied as a measure of hyper conjugation resulting in a stabilizing effect. Second-order perturbation theory can be used to describe the stabilization energies of these interactions, E(2), associated with delocalization i → j and is estimated as $E(2) = -qj\ F(i,j)^2/(\varepsilon i-\varepsilon j)$, where qj is the donor orbital occupancy, εi, εj are diagonal elements (orbital energies) and F(i,j) is the off-diagonal NBO Fock matrix elements.

The E(2) values are summarized in Table 4. Table 4 shows that E(2) in the case of the phenol…ZSM-5 and phenol…Al-ZSM-5 adsorption complexes is larger than that of benzene…ZSM-5 and benzene…Al-ZSM-5 adsorption complexes. Inspection of these energies indicates that E(2) values well correlate with the strength of hydrogen bonding. More values of E(2) were obtained in the phenol adsorption complexes compared to benzene complexes.

Table 4

NBO analysis of donor–acceptor interactions in adsorption complexes showing stabilization energy E(2) values (kJ/mol) at the M06-2X/DZVP2 level of theory, hydrogen bonding energies (E_{HB}) values (kJ/mol) obtained from AIM analysis and main contributions to the adsorption energy (kJ/mol) at the M06-2X/6-311++G** level of theory.

adsorption complexex	donor…acceptor	E_{HB}	E(2)	ΔE_{int}	ΔE^{def}	$\Delta E'_{ads}$	ΔE_{ads}

8T-ZSM-5...Benzene	C_B-H_B…O_{Z1}	-8.64	0.84	-26.44	0.95	-25.49	-34.18
8T-Al-ZSM...5-Benzene	O_{Z1}-H_Z…л	-11.70	0.59	-39.37	2.77	-36.60	-47.79
	C_B-H_B…O_{Z2}	-8.72/-11	1.25				
8T-ZSM-5...Phenol	O_P-H_P …O_{Z1}	-24.7	2.84	-48.24	4.63	-43.61	-59.09
8T-Al-ZSM-5...Phenol	O_{Z1}-H_Z…O_P	-87.90	9.62	-91.25	20.38	-70.87	-105.02
	O_P-H_P…O_{Z2}	-40.10	1.97				

Finally, the adsorption energy, ΔE_{ads}, of benzene and phenol on the zeolites was considered as the energy difference between the absorbed complex system and the total energy of separated fragments as follows:

$$\Delta E_{ads} = E_{complex} - (E_{benzene/phenol} + E_{zeolite}) \quad (3)$$

Where $E_{complex}$ represents the single-point energy of the optimized adsorption complex while $E_{zeolite}$ and $E_{benzene/phenol}$ are the single-point energies of the optimized bare zeolite, separate benzene or phenol, respectively.

The total adsorption energy ($\Delta E'_{ads}$) is assumed as follows:

$$\Delta E'_{ads} = \Delta E_{int} + \Delta E_{def} \quad (4)$$

In which ΔE_{int} represents the total energy consisting the hydrogen bonds and dispersive interactions which is currently calculated as follows:

$$\Delta E_{int} = E_{complex} - (E^S_{benzene/phenol} + E^S_{zeolite}) \quad (5)$$

where $E^S_{zeolite}$ and $E^S_{benzene/phenol}$ are the single-point energies of the zeolite and adsorbate, respectively, at the configurations of host/guest system having no further structural optimization. The ΔE_{def} term represents the deformations of both zeolite and adsorbate molecules which is often separately calculated as follows:

$$\Delta E^{def}_{zeolite} = E^S_{zeolite} - E_{zeolite} \quad (6)$$

$$\Delta E^{def}_{benzene/phenol} = E^S_{benzene/phenol} - E_{benzene/phenol} \quad (7)$$

Counterpoise calculations were carried out at M06-2X/6-311++G** level to evaluate how calculated adsorption energies are affected by the basis set superposition error (BSSE) [59]. The various contributions of adsorption energy obtained at the M06-2X/6-311++G** level of theory are summarized in Table 4. According to obtained data, the deformation energy is more prominent for Al-ZSM-5...Phenol adsorption complex compared to other adsorption complexes that can be due to the stronger hydrogen bonding in Al-ZSM-5...Phenol.

Comparing $\Delta E'_{ads}$ and ΔE_{ads} values reported in Table 4, the difference between them is attributed to basis set superposition error (BSSE) which is neglected in $\Delta E'_{ads}$.

It is worth mentioning that the energy calculation with different analysis obey the similar trend from hydrogen bonding strength standpoint.

Comparing the performance of applied functionals, their obtained data across the adsorption complexes are summarized in Fig. 3 and 4, including the absolute adsorption energy and absolute chemical shift of atoms, the atoms with available experimental chemical shift, respectively, obtained through B3LYP, *w*B97XD, M06-2X functionals. M06-2X and *w*B97XD noticeably improve the accuracy of dispersion energy estimation for systems containing hydrogen-bonding. From Fig. 3 and 4, the M06-2X functional has a higher capability to show and distinguish the dispersion phenomenon in noncovalent interactions compared to *w*B97XD and B3LYP. The obtained findings are in agreement with previous works describing noncovalent interactions in host/guest systems [33, 34, 36, 62].

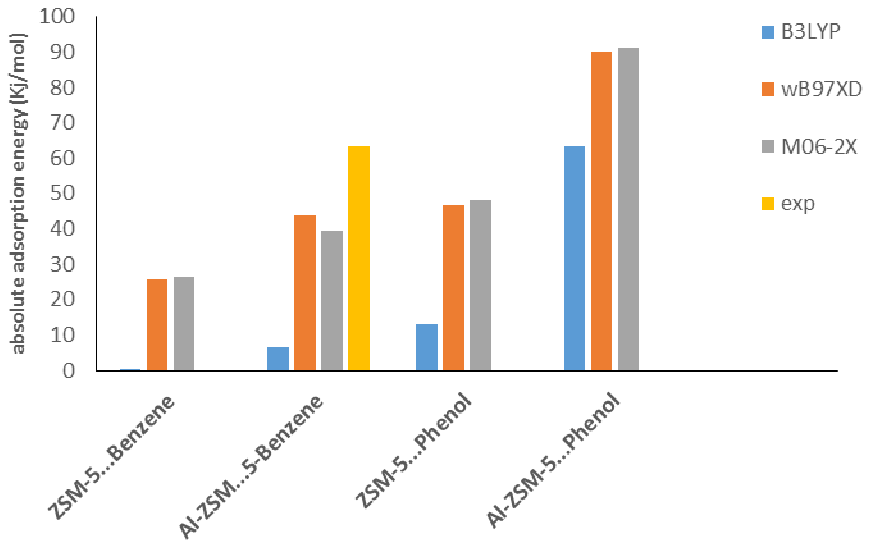

Fig. 3. Calculated and experimental absolute adsorption energies of applied functionals of benzene…ZSM-5, benzene…Al-ZSM-5, phenol…ZSM-5, and phenol…Al-ZSM-5 complexes.

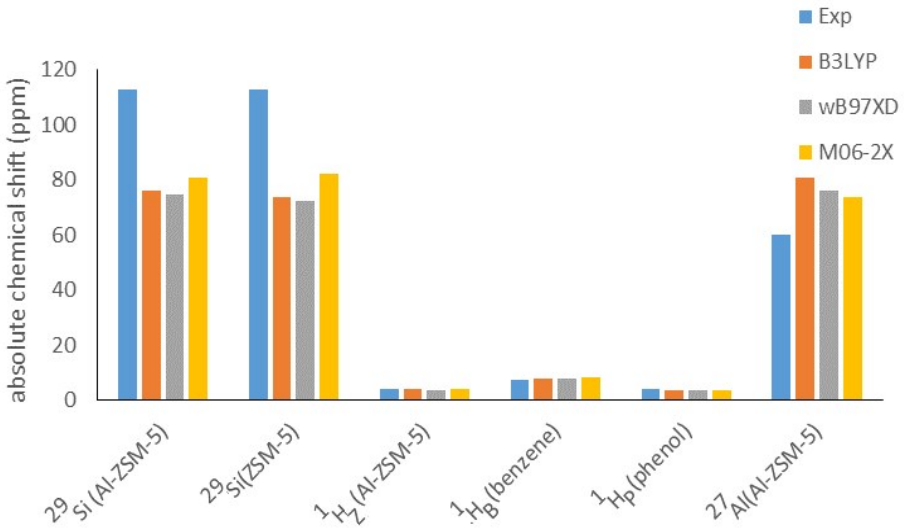

Fig. 4. Calculated and experimental ^{29}Si, ^{27}Al, $^{1}H_Z$, $^{1}H_B$, $^{1}H_P$ absolute chemical shift of applied functionals of benzene, phenol, ZSM-5, and Al-ZSM-5.

CONCLUSION

DFT study was carried out to shed some light on the intermolecular hydrogen bonds in the adsorption complex of the 8T cluster model of ZSM-5 and Al-ZSM-5 catalysts with benzene

and phenol comparatively through B3LYP, M06-2X, and *w*B97XD functionals employing 6-311++G** standard basis set. The computed geometry parameters display one and two types of intermolecular hydrogen bonding possibilities in the guest-ZSM-5 and guest-Al-ZSM-5 complexes, respectively. The C-H…O and O-H…л hydrogen bonds are recognized in the complex formation of benzene adsorbate zeolites. Compared to popular B3LYP functional, M06-2X offered a highly improved performance to concern the noncovalent interactions. All the predicted hydrogen bonds are confirmed via NMR, NQR, NBO, and QTAIM techniques. Variations of adsorption energy, isotropic chemical shifts, δ_{iso}, of ^{1}H, ^{17}O, ^{27}Al, and ^{29}Si atoms contribute to the hydrogen bonding as well as quadrupole coupling constant, C_Q, and asymmetry parameter, η_Q. ^{2}H, ^{17}O, and ^{27}Al atoms are well correlated with the strength of hydrogen bonding. The formation of a hydrogen bond between a surface hydroxyl group and an adsorbed molecule leads to an enhanced isotropic ^{1}H and ^{17}O NMR chemical shift whereas C_Q values of corresponding atoms decrease. Although Al and Si do not participate directly in the interactions, they are affected by these interactions resulting in alternations in NMR and NQR parameters. The total electronic density, $\rho(r_c)$, the Laplacian of electron density, $\nabla^2\rho(r_c)$ and energy density (H) estimated by AIM calculations, show that hydrogen bonds in the phenol…Al-ZSM-5 adsorption complex are partially covalent in nature. The differences in the adsorption behavior between benzene and phenol on the ZSM-5 and Al-ZSM-5 are attributed to the differences in types of interactions. Finally, Al-ZSM-5 appears to be an efficient adsorbent for phenol and benzene.

REFERENCE

1. J. Kärger and D. M. Ruthven, *Diffusion in zeolites and other microporous solids*, Wiley, 1992.
2. S. Kulprathipanja, *Zeolites in industrial separation and catalysis*, John Wiley & Sons, 2010.
3. R. Xu, W. Pang, J. Yu, Q. Huo and J. Chen, *Chemistry of zeolites and related porous materials: synthesis and structure*, John Wiley & Sons, 2009.
4. B. Smit and T. L. M. Maesen, *Chemical Reviews*, 2008, **108**, 4125-4184.

5. J. O'Brien-Abraham, M. Kanezashi and Y. S. Lin, *Journal of Membrane Science*, 2008, **320**, 505-513.
6. M. Petryk, S. Leclerc, D. Canet and J. Fraissard, *Catalysis Today*, 2008, **139**, 234-240.
7. M. F. Fellah, I. Onal and R. A. van Santen, *The Journal of Physical Chemistry C*, 2010, **114**, 12580-12589.
8. E. J. M. Hensen, Q. Zhu, R. A. J. Janssen, P. C. M. M. Magusin, P. J. Kooyman and R. A. van Santen, *Journal of Catalysis*, 2005, **233**, 123-135.
9. A. Reitzmann, E. Klemm and G. Emig, *Chemical Engineering Journal*, 2002, **90**, 149-164.
10. G. Yang and L. Zhou, *Catalysis Science & Technology*, 2014, **4**, 2490-2493.
11. N. Hansen, T. Kerber, J. Sauer, A. T. Bell and F. J. Keil, *Journal of the American Chemical Society*, 2010, **132**, 11525-11538.
12. R. H. Crabtree, O. Eisenstein, G. Sini and E. Peris, *Journal of Organometallic Chemistry*, 1998, **567**, 7-11.
13. F. C. Francisco Sánchez-Viesca, Reina Gómez, Martha Berros, *American Journal of Chemistry*, 2012, **2**, 343-346.
14. I. R. a. J. e. E. Ibon Alkorta, *Chemical Society Reviews*, 1998, **27**.
15. M. L. Huggins, *The Journal of Organic Chemistry*, 1936, **1**, 407-456.
16. G. R. Desiraju and T. Steiner, *The weak hydrogen bond: in structural chemistry and biology*, Oxford university press, 2001.
17. T. P. Das and E. L. Hahn, *Nuclear quadrupole resonance spectroscopy*, Academic Press, New York, 1958.
18. N. Hadipour and S. Javadian, *Journal of Molecular Structure*, 2000, **525**, 129-134.
19. S. Javadian and R. Araghi, *Journal of Molecular Graphics and Modelling*, 2009, **27**, 620-627.
20. M. J. Duer, *Solid state NMR spectroscopy: principles and applications*, John Wiley & Sons, 2008.
21. F. Ektefa, M. Anafche and N. L. Hadipour, *Computational and Theoretical Chemistry*, 2011, **977**, 1-8.
22. N. V. Sidwich, *The Electronic Theory of Valency*, Clarendon, Oxford, 1972.
23. C. Raksakoon and J. Limtrakul, *Journal of Molecular Structure: THEOCHEM*, 2003, **631**, 147-156.
24. R. Rungsirisakun, B. Jansang, P. Pantu and J. Limtrakul, *Journal of Molecular Structure*, 2005, **733**, 239-246.
25. P. M. Esteves and B. Louis, *The Journal of Physical Chemistry B*, 2006, **110**, 16793-16800.
26. Z. Yang, G. Yang, X. Liu and X. Han, *Catalysis Letters*, 2013, **143**, 260-266.
27. E. A. P. G. Li, R.A. van Santen, Z. Feng , C. Li and E.J.M. Hensen, *Journal of Catalysis* 2011, **284**, 194–206.
28. H. van Koningsveld, H. van Bekkum and J. C. Jansen, *Acta Crystallographica Section B*, 1987, **43**, 127-132.
29. A. Zheng, H. Zhang, L. Chen, Y. Yue, C. Ye and F. Deng, *The Journal of Physical Chemistry B*, 2007, **111**, 3085-3089.
30. D. Yi, H. Zhang and Z. Deng, *Journal of Molecular Catalysis A: Chemical*, 2010, **326**, 88-93.
31. S. Yuan, J. Wang, Y. Li and H. Jiao, *Journal of Natural Gas Chemistry*, 2003, **12**, 93-97.
32. M. W. Schmidt, K. K. Baldridge, J. A. Boatz, S. T. Elbert, M. S. Gordon, J. H. Jensen, S. Koseki, N. Matsunaga, K. A. Nguyen, S. Su, T. L. Windus, M. Dupuis and J. A. Montgomery, *Journal of Computational Chemistry*, 1993, **14**, 1347-1363.
33. S. Grimme, *Wiley Interdisciplinary Reviews: Computational Molecular Science*, 2011, **1**, 211-228.
34. Y. Zhao and D. G. Truhlar, *Theoretical Chemistry Accounts*, 2008, **120**, 215-241.
35. I. N. Levine and P. Learning, *Quantum chemistry*, Pearson Prentice Hall Upper Saddle River, NJ, 2009.

36. J. Van der Mynsbrugge, K. Hemelsoet, M. Vandichel, M. Waroquier and V. Van Speybroeck, *The Journal of Physical Chemistry C*, 2012, **116**, 5499-5508.
37. E. A. C. Lucken, *Nuclear Quadrupole Coupling Constants,* , Academic Press, London, 1969.
38. P. Pyykkö, *Molecular Physics*, 2001, **99**, 1617-1629.
39. J. F. H. a. P. P. K. Wolinski, *Journal of American Chemical Society*, 1990 **112** 8251-8260.
40. S. Sternhell, *Organic Magnetic Resonance*, 1983, **21**, 770-770.
41. J. K. M. Cambridge, *Magnetic Resonance in Chemistry*, 1987, **25**, 280-280.
42. S. Sklenak, J. Dědeček, C. Li, B. Wichterlová, V. Gábová, M. Sierka and J. Sauer, *Angewandte Chemie International Edition*, 2007, **46**, 7286-7289.
43. L. A. C. a. F. W. A.E. Reed, *Chemical Reviews*, 1988, **88**, 899-926.
44. J. S. F. Biegler-König, D. Bayles, *Journal of Computational Chemistry*, 2001.
45. H. Huo, L. Peng and C. P. Grey, *The Journal of Physical Chemistry C*, 2011, **115**, 2030-2037.
46. D. W. J. C. a. J. A. S. S. E. G. Cox, *mathematical physics and engineering science*, 1958, **247**, 1-21.
47. G. A. Jeffrey, *An Introduction to Hydrogen Bonding*, Oxford University Press, Oxford, 1997.
48. U. Koch and P. L. A. Popelier, *The Journal of Physical Chemistry*, 1995, **99**, 9747-9754.
49. S. K. Panigrahi and G. R. Desiraju, *Proteins: Structure, Function, and Bioinformatics*, 2007, **67**, 128-141.
50. A. Zheng, L. Chen, J. Yang, Y. Yue, C. Ye, X. Lu and F. Deng, *Chemical communications*, 2005, 2474-2476.
51. A. Zheng, L. Chen, J. Yang, M. Zhang, Y. Su, Y. Yue, C. Ye and F. Deng, *The Journal of Physical Chemistry B*, 2005, **109**, 24273-24279.
52. C. Tuma and J. Sauer, *Chemical physics letters*, 2004, **387**, 388-394.
53. M. M. Mestdagh, W. E. Stone and J. J. Fripiat, *The Journal of Physical Chemistry*, 1972, **76**, 1220-1226.
54. D. Pavia, G. Lampman, G. Kriz and J. Vyvyan, *Introduction to Spectroscopy*, Cengage Learning, 2008.
55. Y. Jiang, J. Huang, W. Dai and M. Hunger, *Solid State Nuclear Magnetic Resonance*, 2011, **39**, 116-141.
56. S. S. J. De˘dec˘ek, C. Li, B. Wichterlová, V. Gábová, J. Brus, M. Sierka and J. Sauer, Paris, 2008.
57. W. C. Conner, R. Vincent, P. Man and J. Fraissard, *Catalysis letters*, 1990, **4**, 75-83.
58. D. Freude, H. Ernst and I. Wolf, *Solid State Nuclear Magnetic Resonance*, 1994, **3**, 271-286.
59. R. F. Bader, *Atoms in molecules*, Wiley Online Library, 1990.
60. I. Rozas, I. Alkorta and J. Elguero, *Journal of the American Chemical Society*, 2000, **122**, 11154-11161.
61. E. Espinosa, E. Molins and C. Lecomte, *Chemical physics letters*, 1998, **285**, 170-173.
62. B. Boekfa, P. Pantu, M. Probst and J. Limtrakul, *The Journal of Physical Chemistry C*, 2010, **114**, 15061-15067.

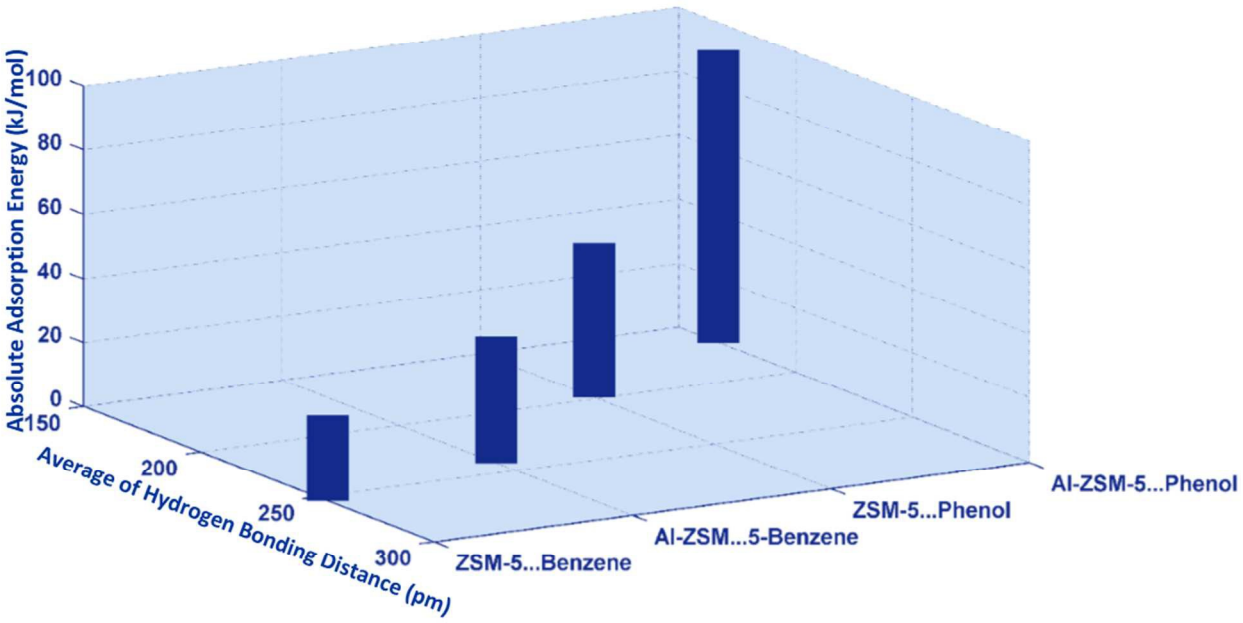

The adsorption behavior of benzene and phenol on the zeolite are attributed to the differences in the strength of their interactions.